University of Texas at El Paso

ScholarWorks@UTEP

2023-05-01

Additive Manufacturing Of Binary And Ternary Shape Memory Polyester Blends As A Pathway Towards High Entropy Polymer Systems.

Luis Eduardo Lares Carrillo
University of Texas at El Paso

ADDITIVE MANUFACTURING OF BINARY AND TERNARY SHAPE MEMORY

POLYESTER BLENDS AS A PATHWAY TOWARDS HIGH ENTROPY POLYMER

SYSTEMS.

LUIS EDUARDO LARES CARRILLO

Master's Program in Metallurgical and Materials Engineering

APPROVED:

David Roberson, Ph.D., Chair

Robert C. Roberts, Ph.D.

Sylvia Natividad-Diaz, Ph. D.

Stephen L. Crites, Jr., Ph.D.
Dean of the Graduate School

1. Dedication

This work is dedicated in the first place to my mother who has always supported me in every way possible and has been there for me in the good and bad times and always gives the motives to keep going. I would also dedicate this work to God since it has been giving me its blessing and always takes care of me. I also dedicate this work to my family that is always there for me and supports me. This has been a long path and want to thank all the people that were here with me, my friends, my girlfriend that also has supported me and was the reason for me to be where I am thanks to all of you.

ADDITIVE MANUFACTURING OF BINARY AND TERNARY SHAPE MEMORY

POLYESTER BLENDS AS A PATHWAY TOWARDS HIGH ENTROPY POLYMER

SYSTEMS.

by

Luis Eduardo Lares Carrillo

THESIS

Presented to the Faculty of the Graduate School of

The University of Texas at El Paso

in Partial Fulfillment

of the Requirements

for the Degree of

MASTER OF SCIENCE

Department of Metallurgical, Materials and Biomedical Engineering

THE UNIVERSITY OF TEXAS AT EL PASO

May 2023

2. Acknowledgements

I would like to thank Dr. David Roberson for being my mentor and friend through all my path at The University of Texas at El Paso, I am grateful, to Dr. Stella Quinones because she is the reason that I studied in the MME department and she helped me a lot through all my time in the department in every aspect that she could. I would also like to acknowledge the Consejo Nacional de Ciencia y Tecnología (CONACyT) from Mexico that sponsored the first years of my degree and the National Science Foundation (NSF) under grant number CMMI 2227573 that funded me as well. To my lab partners Truman Word, Diego Bermudez and Jose Salazar that helped me every time I had a doubt.

3. Abstract

The purpose of this work is to incorporate additive manufacturing technology (AM) in the development of shape memory polymer blends. Two polyester blend systems were developed, one binary and the other ternary. The binary blend consisted of polycaprolactone (PCL) and thermoplastic polyurethane (TPU) and the ternary blend was composed of PCL, TPU and polylactic acid (PLA). Test specimens were fabricated with the AM technology of fused filament fabrication (FFF). Several tests were performed to characterize the mechanical and shape memory properties. A dynamic mechanical analyzer (DMA) was first used to establish the shape recovery temperature. Tensile testing was carried out to determine the ultimate tensile strength (UTS) an % elongation (%El) values. Tensile testing was also used to determine the critical shape memory [properties, namely the shape recovery ratio (R_r) and shape fixation ratio (R_f). A key aspect of this work also involves the emerging materials science premise of high entropy materials and demonstrates how ternary blends can open the way for high entropy shape memory polymers. The shape memory performance of the two blend systems is also compared. This work also explores the self-healing capability of TPU/PCL and TPU/PCL/PLA blend systems. Additionally, the effect of raster pattern on the mechanical and shape memory properties is also made. Scanning electron microscopy (SEM) was used to perform fracture surface analysis and a difference between material type and raster pattern was also made.

4. Table of Contents

5. List of Tables

6. List of Figures

1. Chapter 1: Introduction

Shape memory polymers (SMP)s have the ability to recover their original shape after a stimulus is applied. This stimulus could be heat, force, electric impulse etc. In the case of heat-activated SMPs temporary shape can be obtained when the specimen is deformed and then recovered by heating it above its glass transition temperature (T_g) [1]. Interest in shape memory polymers has increased over the past few years and its applications has been applied in different fields such as aerospace, biomedical and automotive since the late 1990s and its applications from wound sutures to aerospace components have increased since then [2] [3]. When SMPs are combined with additive manufacturing (AM), also referred to as 3D Printing, the terminology "4D Printing" is sometimes used [1,4]. This combination of advanced materials and advanced manufacturing platforms allows the obtention of different shapes for almost every application in a lot of fields in the industry [3] [5].

Polycaprolactone (PCL) and thermoplastic polyurethane (TPU) both have shape memory properties on their own [6] however, there is not a large body of work in literature pertaining to blends composed of these two constituents. Work performed by Wang et al. explored aspects of PCL/TPU blends and their potential as shape memory polymers and ability to act in a similar manner such as metal shape memory alloys. [7]. In addition, this work addresses the importance of high entropy polymer blends using PCL and TPU combined with polylactic acid (PLA) in the creation of a ternary blend. These materials were chosen as blend constituents because PLA, TPU and PCL are polymers that can be blend easily without the necessity of involving solvents or chemical compatibilizers [8] due to similarities in the Hildenbrand solubility parameter (δ) [4] and similarities in their

1

molecular structure (they are all long chain polyesters). PCL and TPU have a wide variety of applications for example they are used as self-knotting sutures [9] and blends composed of PCL and TPU combined with additives in order to enhance their properties. One of the additives that has been added is multi-wall carbon nanotubes (MWCNT)s [10] where it was found that the addition of MWCNTs allowed shape memory and self-healing functionality upon the exposure to ultraviolet light. Polylactic acid (PLA) is one of the most common polymers used for additive manufacturing and have a wide applications range this polymer can be used for printing at home to even print scaffolds for cell growth due to its biocompatibility [11] [12]. Usually when PLA is added to PCL the resultant mechanical properties are improved and according to Ebrahimi et al. [13], the local acidification is reduced hence the inflammatory response as well when used in tissue engineering applications.

The premise of polymer high entropy blends (HEB)s comes from the same concept of high entropy metal alloys (HEA)s, and example of which was demonstrated by Yeh et al. in 2004 [14] where more than two metals are combined in order to improve its properties. Haase, et al. [15] used 3D printing technology to create a high entropy alloy using Co-Cr-Fe-Mn-Ti and used the laser metal deposition technique, Selective Laser Melting (SLM), to manufacture the alloy and showed an improvement in the properties of the already existing alloys . There are other attempts to increase the knowledge in the field of HEA's such as work performed by Popov, et al. [16], who fabricated components from Al0.5CrMoNbTa0.5 using electron beam melting (EBM) technology, but couldn't achieve a homogeneous microstructure. However, the work of Popov, et al. was an important advancement for the upcoming technology due to it demonstrate that a multi-

2

constituent alloy can be used for additive manufacturing but would need a post processing to reduce the defects caused by the manufacturing process; hence, it set a precedent.

The combination of different types in the creation of a high entropy polymer blend (HEPB) has been demonstrated in literature, but there is currently not a large body of work. A noteworthy example was demonstrated by Huang et al. [17] who combined 5 types of polymers that were dissimilar, polystyrene (PS), poly(methyl methacrylate) (PMMA), polycarbonate (PC), polyvinylpyrrolidone (PVP,), and polyisoprene (PIP) using a solvent. Key aspects related to the difficulties in creating HEPBs were pointed out in this work, such as "de-mixing of polymers" due to a decrease in heat of mixing that trends linearly with the number of constituents [17]. Melt compounding of binary, ternary, and quaternary polyamide blends was demonstrated by Hirai, et al. [18] where mixing of the materials was facilitated by an exchange reaction between the individual blend constituents.

In the work here we rely upon similarities in polymer characteristics to facilitate blending. PLA was made to the PCL and TPU blend in order to create ternary blend which could be considered as a HEB as the constituents were added in equal amounts. The blend was evaluated for its shape memory properties and its self-healing effect. Self-Healing effect is the capability of a material to recover from physical damage [19] which usually comes along with the SME [20] [21]. PLA was picked due to its solubility parameter which ranges between 20.7 and 19.9 20 $MPa^{1/2}$ [22] while PCL varies from 15.8 to 21.2 [23] and the solubility parameter for TPU is in the order of 20 $MPa^{1/2}$ [24] . As mentioned above, in addition to similar solubility parameters, all three materials studied in this work are long chain linear polyesters.

Shape memory properties can be quantified using different formulas to calculate the critical parameters, fixation ratio (R_f), the ability of a material to hold a temporary shape, and shape recovery ratio (R_r) the ability of a material to return to the permanent or "programmed" shape. These parameters are calculated with the following equations [4] [1] [25].

$$R_f(\%) = \frac{\epsilon_u}{\epsilon_m} \times 100\ \% \qquad (1)$$

$$R_r(\%) = \frac{\epsilon_m - \epsilon_p}{\epsilon_m} \times 100\ \% \qquad (2)$$

Where ϵ_m is the maximum strain that the specimen can achieve when is pulled to its 100 % of its own length, ϵ_u is the elongation of the specimen after the specimen is unloaded from the tension that was applied, and ϵ_p is the elongation after recovery process which can be different stimuli whether is heat, electromagnetic, moisture etc. [25]. Previous work conducted by our group has involved several melt-compounded shape memory polymer blends. Work by Chávez et al. [1] performed a full property and microstructural characterization of a blend system composed of acrylonitrile butadiene styrene (ABS) and styrene ethylene butylene styrene with a maleic anhydride graft (SEBS-g-MA) and proved by way of scanning transmission electron microscopy (STEM) that the phases were aligned by the FFF process and that this alignment had an influence on the shape memory properties. Further work conducted by Quiñones, et al. [4] characterized the shape memory properties of a PLA/TPU blend as well as a PLA/SEBS-g-MA blend and compared the effect of the fabrication method of fused filament fabrication (FFF) to injection molding on shape memory properties and found that the FFF process positively influenced shape memory performance, most likely due to the phase

alignment. It is important to note that the ABS/SEBS-g-MA blend and the PLA/SEBS-g-MA blend were immiscible due to differences in miscibility parameter and their blending was facilitated by the maleic anhydride graft. On the other hand, PLA and TPU have similar structures and miscibility parameters and we proved that though two phases were observed, that these phases were more interspersed with uniform domain sizes as compared to either ABS/SEBS-g-MA or PLA/SENS-g-MA [4,26]. We have documented in other works that using the FFF process to align the phases in a direction parallel to the direction of applied stress provides optimum shape memory performance in terms of the shape memory properties, namely R_r and R_f [1,4,25,27].

The self-healing effect was also observed during this research. The concept of self-healing is similar to the shape memory process where shape recovery can be a component of the healing process. An analogy is the recovery from physical damage by biological organisms. In nature, this process is usually slow, for example human skin self-heals via cell growth however, self-healing can also occur in synthetic polymers [28] as we have observed here. This effect has a wide variety of applications such as soft robotics, microelectronics and biomedicine. The healing ability of PCL, stems from its low melting temperature, according to Bhattacharya et al. [29], which allows PCL or the PCL phase in a mixture to reflow and essentially act as an adhesive, thus repairing damage. The self-healing effect in polymers is generally facilitated by a thermal effect due to the increased temperature allowing a more rapid relaxation of the polymer chains and this enables the fibers rearrange to their original state [30]. This effect can occur with different stimulus such as photo-induced healing, recombination of chain ends, molecular

5

interdiffusion, and thermally reversible crosslinked polymers [31]. These properties are important due to the loss of structural capacity or functionality overtime [32].

Self-healing efficiency (R) can be defined based on a variety of physical properties and comparing "healed" to pristine specimens in a ratio equation as was demonstrated by Wool and O'Connor [33]. The physical property can be Young's Modulus (E), percent elongation (ε) or ultimate tensile strength (σ):

$$R(E) = \frac{E_{cut}}{E_{pristine}} \times 100\% \qquad (3)$$

$$R(\varepsilon) = \frac{\varepsilon_{cut}}{\varepsilon_{pristine}} \times 100\% \qquad (4)$$

$$R(\sigma) = \frac{\sigma_{cut}}{\sigma_{pristine}} \times 100\% \qquad (5)$$

Shape memory and self-healing properties are important due to the constant plastic pollution that affects the environment. A positive environmental effect could be realized by implementing polymer materials could be easily repaired rather than thrown away and replaced with another polymer component [34]. The realization of waste reduction would then be two-fold as you would not create waste by throwing a component away and you would also not create future waste by replacing the damaged part.

According to Liu and Chuo, [35] self-healing polymers can be categorized in two groups "Autonomous" and "Stimuli-responsive" the autonomous category usually only happens once while the stimuli-responsive can be performed repeatedly. Besides there are other techniques where different agents can be added to the blend in order to increase that properties [19]. However, Bode et al. also categorized self-healing polymers into Extrinsic self-healing that is based on the presence of intentionally added discrete micro encapsulated healing agents and intrinsic healing where is related to the chemical

modification of the polymer base and make it capable of restoring chemical bonds across the damage site [36] [37] [38] [39]. As previously discussed, there are more applications to this effect in the biomedical field where PLA plays a major role as demonstrated by Gupta et al. [40] who demonstrated using a PLA scaffold to regenerate a meniscus tissue with carbohydrate based self-healing interpenetrating network hydrogel.

The work demonstrated here utilizes melt compounding to binary and ternary blends. The materials used, PLA, PCL, and TPU are all biocompatible and could potentially be used in biomedical applications. The comparison between the blends will be to look for the blend that has more elongation and ultimate tensile strength. The key research questions to be answered by this work are:

1) What is the optimum ratio of TPU and PCL in a binary blend?
2) How does the addition of PLA in the creation of a ternary blend impact the mechanical and shape memory properties?
3) Do these new material systems have self-healing capabilities?

2. Chapter 2: Materials and Methods

The binary and ternary polymer blends were created through the process of melt compounding using a Collin twin-screw extruder-compounder (Model ZK 25-T, Collin Lab and Pilot Solutions, Norcross, GA, USA) equipped with a melt pump and belt puller. Filaments were extruded with a target diameter of 2.85 mm in order to be compatible with the FFF machine used in this study. The extrusion parameters are tabularized in Table 2.1. The binary blend was a combination of TPU and PCL and the ternary blend was composed of TPU, PCL, and PLA in equal weight ratios. The PLA used in this work was obtained from NatureWorks, LLC (Ingeo Biopolymer Grade 4043D, NatureWorks, LLC, Minnetonka MN, USA) in pellet form. The TPU used in this work was obtained from NinjaTek (Fenner Precision Polymers, Lititz, PA, USA) and was received in filament form which was later pelletized using a Collin strand pelletizer (Model SP1 Collin Lab and Pilot Solutions, Norcross, GA, USA). The PCL used in this work was obtained from Polly Plastics (Midland, MI, USA) and was received in pellet form. Prior to processing, the PLA was dried for 2 hours at 50 °C with air using a compressed air dryer (Micro Dryer CAFM station, Dri-Air Industries, East Windsor, CT, USA). After that, the specimens were fabricated using the FFF manufacturing process with a Lulzbot Taz 5 (Lulzbot, Fargo, North Dakota, USA) with a 0.5 mm diameter nozzle following the machine parameters that are listed in Table 2.2. Table 2.1: Extrusion Parameters in °C. The experimentation process steps can be seen in the following diagram Figure 2.1.

Figure 2.1: Process Steps.

There were three types of specimens printed for the testing procedure, the dog bone-type tensile specimen was based on the ASTM D638 [41] Type V and type IV geometry and was used for the tensile testing process and the 3rd type was a dynamic mechanical analysis sample (DMA) used for the DMA testing. In Figure 2.2.2 the tensile samples type IV and type V are shown.
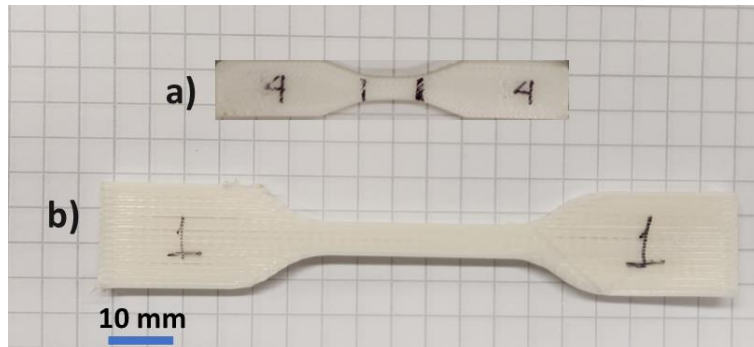

Figure 2.2. Tensile specimens a) Type V and b) Type IV.

Initial experiments focused on the development of the binary blend in terms of weight ratio of each constituent (75 % PCL 25 % TPU, 50 % PCL 50 % TPU, 25 % PCL 75 % TPU). As the ternary blend is intended to be treated as a high entropy blend, only equal parts (by weight) of PLA, PCL, and TPU were studied. The various combinations are tabulated in **Error! Reference source not found.**. The temperature parameters for extrusion were determined based previous studies found in literature [9] [42] [43]. Different types of cooling were needed, air and water cooling, since the stickiness of the PCL made it difficult to extrude and spool. The sample 75 PCL 25 TPU was the blend that needed water to cool. The difference between the HEB and the binary blends were observed in this process due to the extrusion being more stable in the HEB. The FFF was conducted with the parameters obtained in AMFG [44] that can be seen in Table 2.2. Two print raster patterns were used, a longitudinal raster pattern where the print raster's are

in the direction of the length of the specimen and an alternating crisscross pattern where the print raster alternated by 45° for each layer (Figure 2.3). The initial testing of the ternary blends only involved the longitudinal raster pattern as we chose the best performer in terms of tensile testing for further shape memory property testing. As will be seen the best performing binary blend was the 50/50 by weight ratio blend of PCL and TPU. The printed samples were stored zip bags with desiccant to avoid any hygroscopic damage due to moisture [45].

Table 2.1: Extrusion Parameters in °C.

Blends	Zone 1	Zone 2	Zone 3	Zone 4	Zone 5	Zone 6	Cooling Method
75 PCL 25 TPU	155 °C	170 °C	170 °C	170 °C	170 °C	170 °C	Water Quenched
50/50 PCL/TPU	180 °C	180 °C	180 °C	180 °C	180 °C	180 °C	Air
25 PCL 75 TPU	175 °C	175 °C	175 °C	175 °C	175 °C	175 °C	Air
HEB	150 °C	180 °C	180 °C	180 °C	175 °C	175 °C	Air

Table 2.2: Printing Settings.

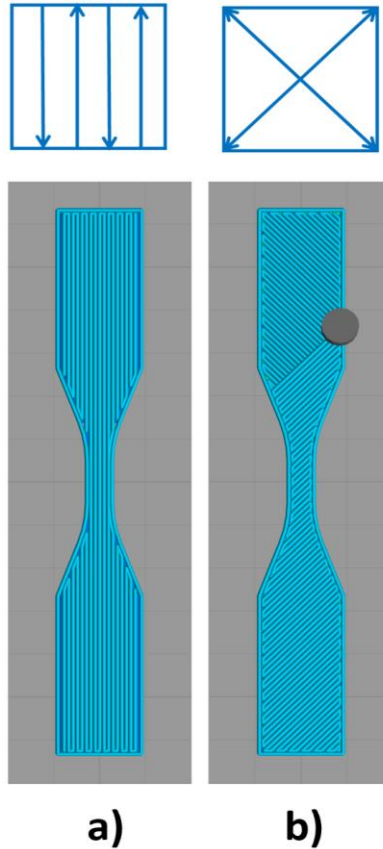| Printer Settings	75 PCL 25 TPU	50/50 PCL/TPU	25 PCL 75 TPU	HEB
Bed Temperature	50°C	50°C	50°C	50°C
Nozzle Temperature	210°C	220°C	225°C	210°C

Figure 2.3. The print raster patterns used in this study: a) longitudinal, and b) 45°.

Specimens for DMA testing were also printed by way of FFF. The instrument used for DMA testing was a PerkinElmer DMA 8000 (PerkinElmer, Waltham, MA, USA). In addition to providing information related to dampening, testing with DMA allowed for the determination the correct recovery temperature, which, in other works performed by our group has been the temperature at which the maximum tan δ occurs. [1,4]. Tensile testing was carried out using a MTS Criterion C-44 tensile testing machine outfitted with an Advantage™ Model AHX 800 extensometer (MTS Systems Corporation, Eden Prairie, MN, USA).

The MTS criterion was then to document tensile properties for our materials. We also wanted to verify that the materials could withstand 100% elongation at room

temperature. In, general our procedure for determining the shape memory properties has been to hold specimens at 100% elongation for a period of 5 min [1,4]. The recovery temperature was 65 °C which was close to all the max tan δ temperature for all materials tested. As mentioned above, the best performing binary blend was the 50% PCL 50 % TPU and we tested this material system again by way of DMA and tensile testing in the other print raster we used, the alternating 45° printing orientation in order to compare with the HEB. The T_g for the binary blend and the HEB was the same according to the DMA testing [46].

The Final tests that were conducted in this effort were performed to determine the self-healing properties of the material systems. This effect can occur with different stimulus such as photo-induced healing, recombination of chain ends, molecular interdiffusion, and thermally reversible crosslinked polymers [31]. These properties are important due to the loss of structural capacity or functionality overtime [32]. For this experiment a squared film was printed using FFF technique with the HEB. First it was printed and then deformed by folding them several times, the orientation used was longitudinal and 45° to see if there is any difference after that it was recovered in hot water at 70 °C to assess its recovery time and condition.

The second test was the "Cut-Test" where a type V sample was cut in the middle and then recovered at 80 °C in the oven. The sample was recovered in a fixture that was 3D printed with PETG that is illustrated in Figure 2.4 below. In Figure 2.5 the set up can be spotted where the jig was closed. In this test the blends that were tested were 50/50 PCL/TPU and HEB and its outcomes were compared one and another to assess its ability to recover. In order to avoid the sample sticking to the jig cooking spray was used as mold

12

release to facilitate the removal of the sample after it was heated. For this experiment both orientations were used to see if there was a difference between both raster patterns.
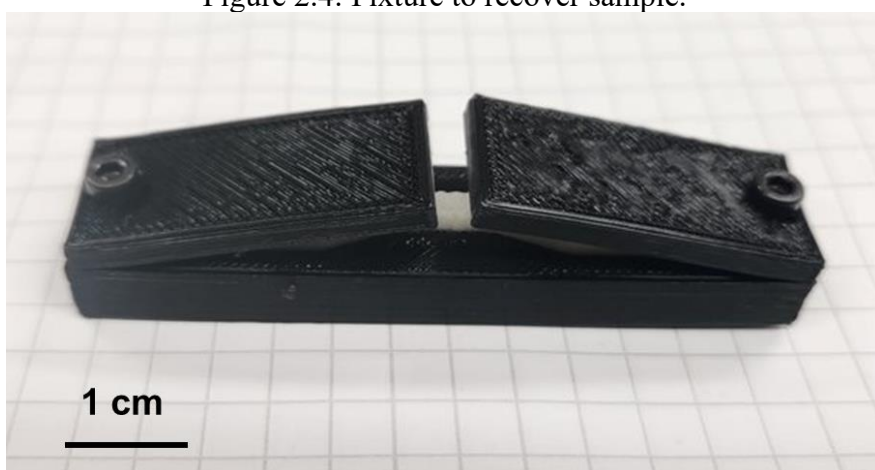

Figure 2.4: Fixture to recover sample.

Figure 2.5: Recovery Set up in the fixture.

3. Chapter 3: Results/Discussion

Rheological Characterization

DMA Testing: On the Figure 3.1 it can be observed the results of the binary blends with different concentrations compared with the HEB. As the PCL concentration was lowered the blend started acting as a more spring since the tan decreased with an increase in PCL. The T_g could be observed simply all of them below 70°C as seen in Table 3.1. DMA Parameters. That is why the temperature picked to recover all the blends was 65°C so all the blends would be above its T_g. On the PCL-TPU blends there was only one option due to the other options for the temperatures were very low hence the blends were tested only in one temperature. In contrast, HEB was indeed able to obtain two temperatures, however both were similar (63 °C and 50 °C) as they are appointed in Figure 3.2 a) and b). This phenomenon occurred only in one orientation due to the curves for the printing orientation changed along longitudinal and 45° raster pattern.

Table 3.1. DMA Parameters

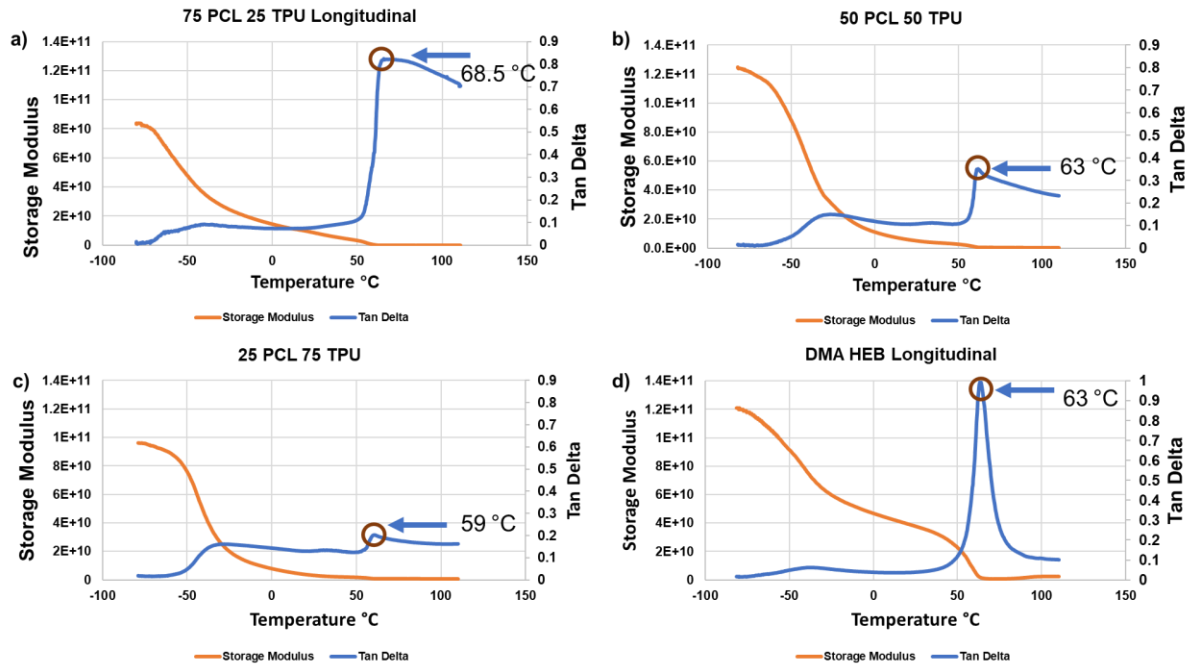| Experimental Group	Max Tan	Temp (°C) (Max tan δ)	Storage Modulus at Glassy Onset	Temp (°C)
75 PCL/25 TPU	0.85	68.5 °C	8.00E+10 Pa	-75 °C
50 PCL/50 TPU Long	0.35	63 °C	1.18E+11 Pa	-70 °C
50 PCL/50 TPU 45	0.57	62.75 °C	7.19E+10 Pa	-65 °C
25 PCL/75 TPU	0.2	59 °C	8.30E+10 Pa	-55 °C
HEB Long	1	63 °C	2.51E+10 Pa	50 °C
HEB 45	0.8	65 °C	6.00E+10 Pa	-65 °C

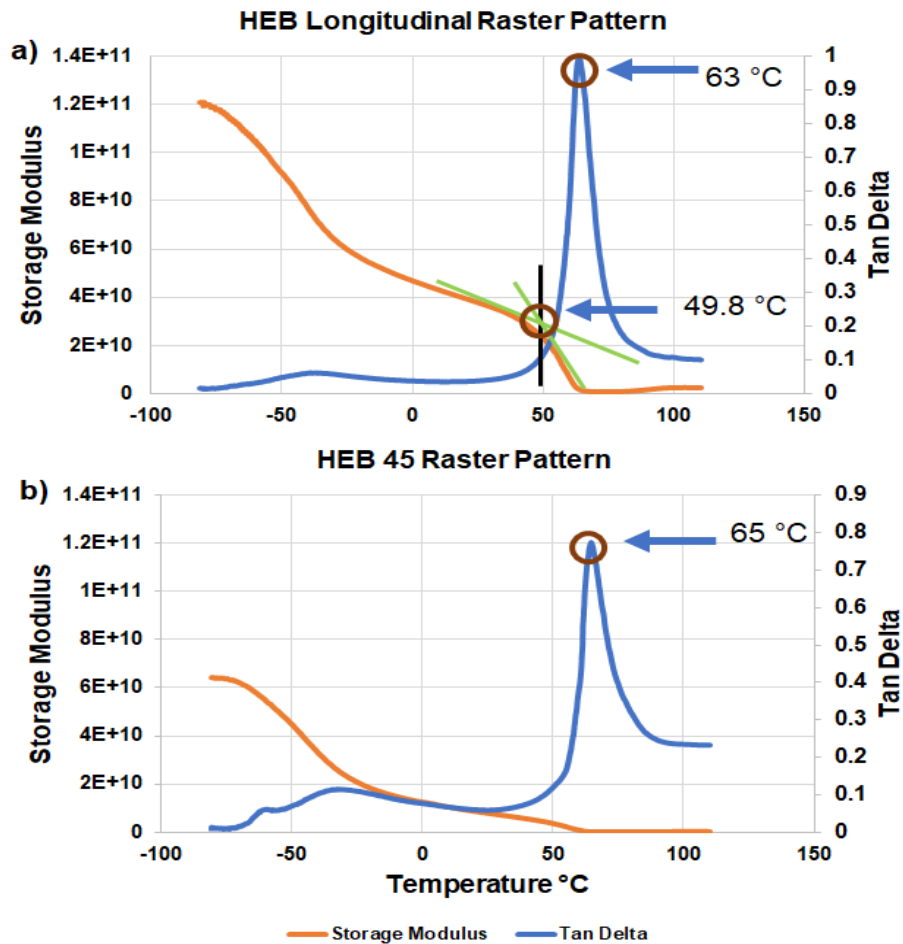Figure 3.1. DMA Testing comparison with normal blends.

Figure 3.2.DMA Results HEB different raster patterns.

MECHANICAL TESTING

The tensile testing was performed first in the normal blends where the most elastic blend would be then compared to the HEB with different raster patterns. For this test two factors were taken in consideration that were % Elongation (%El) and Ultimate Tensile Strength (UTS). The difference in %El and UTS were very noticeable where both highest values were obtained by the blend 50% PCL 50% TPU. This was not an expected result since accordingly to the nature of the TPU with its elongation properties it should add more elasticity to the blend however the least elongated blend was 25% PCL 75% TPU which only achieved up to 1200% elongation whereas the best one could achieve almost 2000+/- 112% elongation moreover in the UTS the 50/50 PCL/TPU blend was the best performer from the first three iterations of a binary blend. These results helped us to determine that the 50/50 PCL/TPU blend was the best performer and we chose this one to be compared it with the HEB blend.
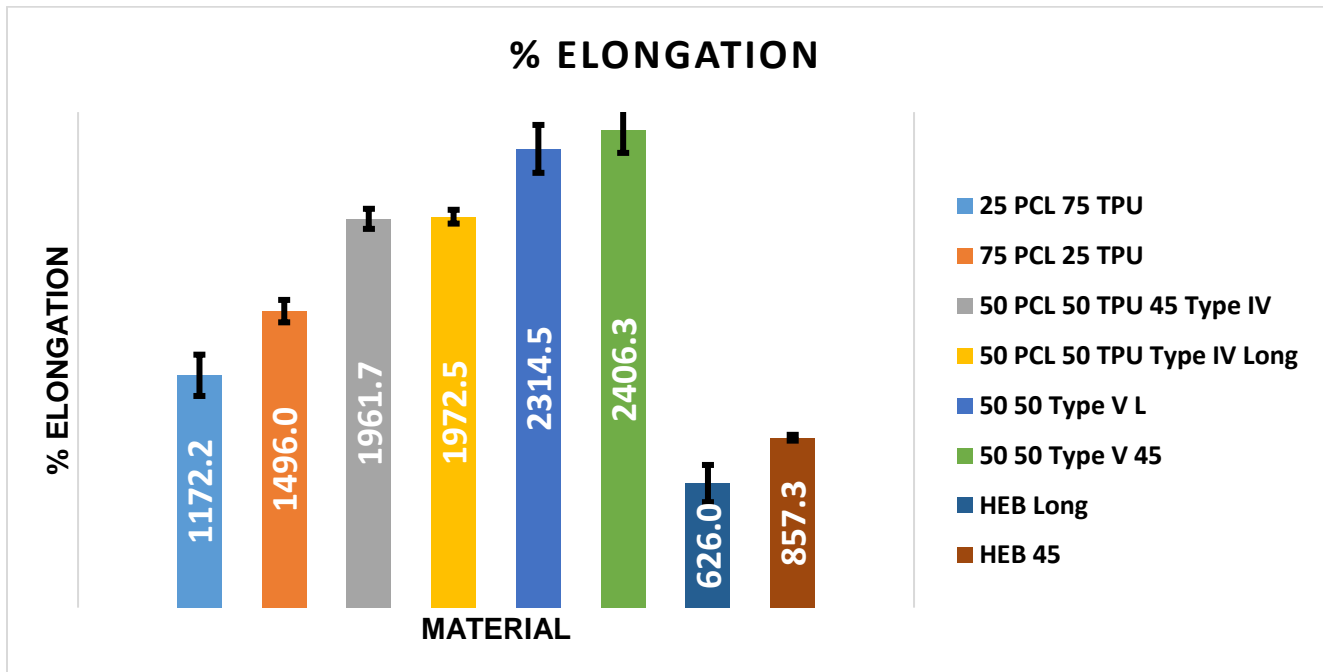

Figure 3.3. % Elongation.

The HEB blend did not overtake the other blends in terms of %El and its result was that it did not elongate to 1000%. However, the %El values were enough to perform shape memory characterization. In contrast with the 50/50 PCL/TPU blend did not exhibit raster pattern sensitivity in terms of %EL, but HEB did where the 45° raster was able to sustain more plastic deformation as more than 2400+/-112. two times compared to the longitudinal orientation as seen in Figure 3.3. In terms of UTS, the HEB could exhibited higher values as compared with the iterations of the binary blend where the average surpass the strongest blend as seen in Figure 3.4 however, on the contrary of the 50/50 PCL/TPU the strongest specimen was the 45° orientation that could withstand an average of 35.9±/-2.04 MPa surpassing the 50/50 PCL/TPU that only could achieve 34.4 MPa. Overall, the rate of UTS oscillates between 15+/-.73 MPa and 35.9+/-2.04 MPa.
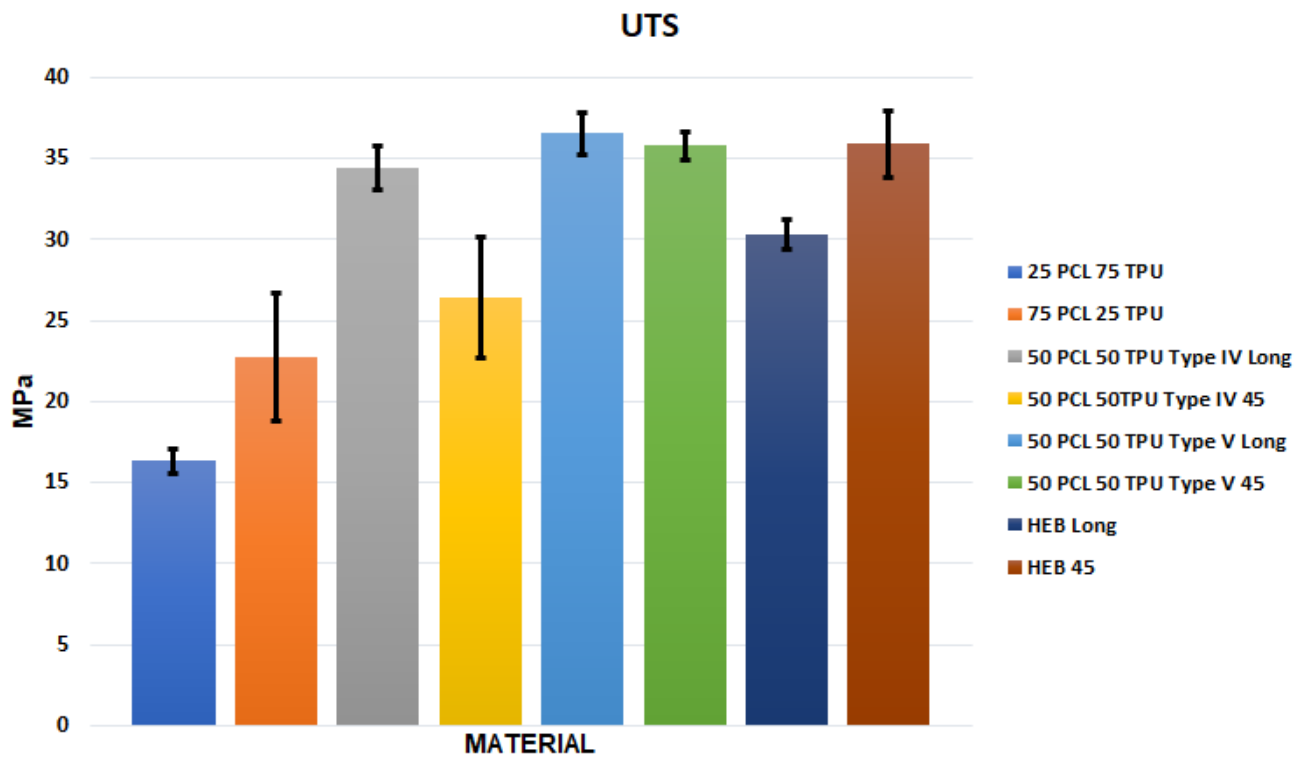

Figure 3.4. Ultimate Tensile Strength.

Characterization of the shape memory properties was performed on all blends but for 50/50 PCL/TPU blend due to material constraints it was performed first in a Type V then in a Type IV shape. The results were that it was easier for 50/50 PCL/TPU to recover its original shape than in the case of the 75/25 PCL/TPU and 25/75 PCL/TPU blends where they were crooked and even though they had best SMI they did not fully recover their shape, so the calculation could not describe the actual behavior of the materials (Figure 3.5). Including shape and the parameters describing the formulas, the best blend in shape memory properties was the binary blend composed of 50/50 PCL/TPU. This is due to the balance between both polymers. The HEB had better results in comparison with the other blends. However, the first try of the SMT the specimen shrank, that is why the HEB Long exceeded the recovery ratio. Not only did they shrink, but they also crooked in such a way that they could not be recovered properly. In order to avoid this situation, the HEB specimens were healed at different times, but the shape was not recovered well either (Figure 3.6 g, and h). After that, it was decided to pre heat the specimens before at 65 ℃ for 5 minutes then cooled down for 2 minutes at room temperature until room temperature was reached. This method worked very well (Figure 3.6 i and j) and had better results than the non-pre heated ones. Non-pre-heated samples at least one of the samples shrank while the pre-heated samples none of them shrank and held a very good shape memory index and recovery ratio. The tensile behavior changed as well in the HEB pre-heated specimens while the longitudinal orientation improved its tensile behavior the 45° orientation decreased the tensile strength a little bit but was better than the normal HEB

longitudinal orientation. This behavior, when the blends have a better performance after a source of heat is applied is usually is known as Polymer Relaxation [47].

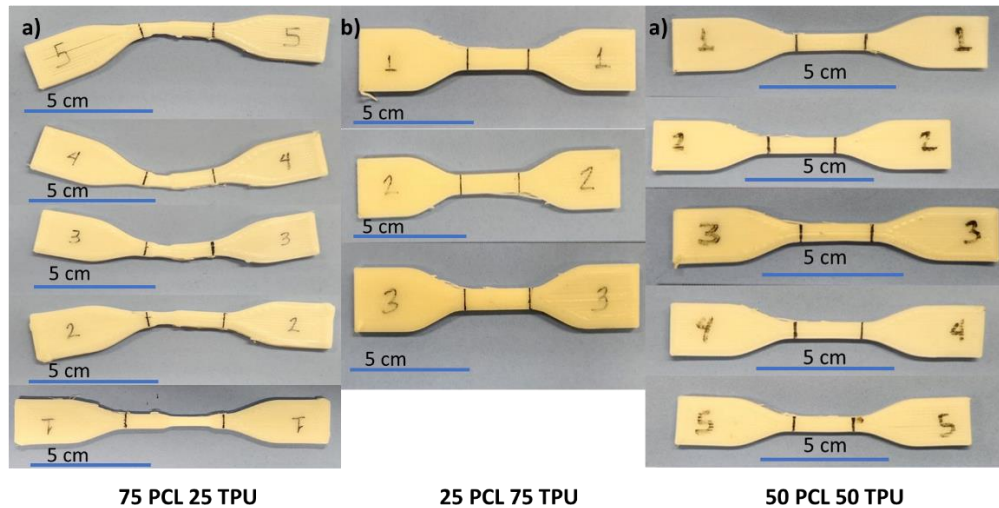75 PCL 25 TPU   25 PCL 75 TPU   50 PCL 50 TPU

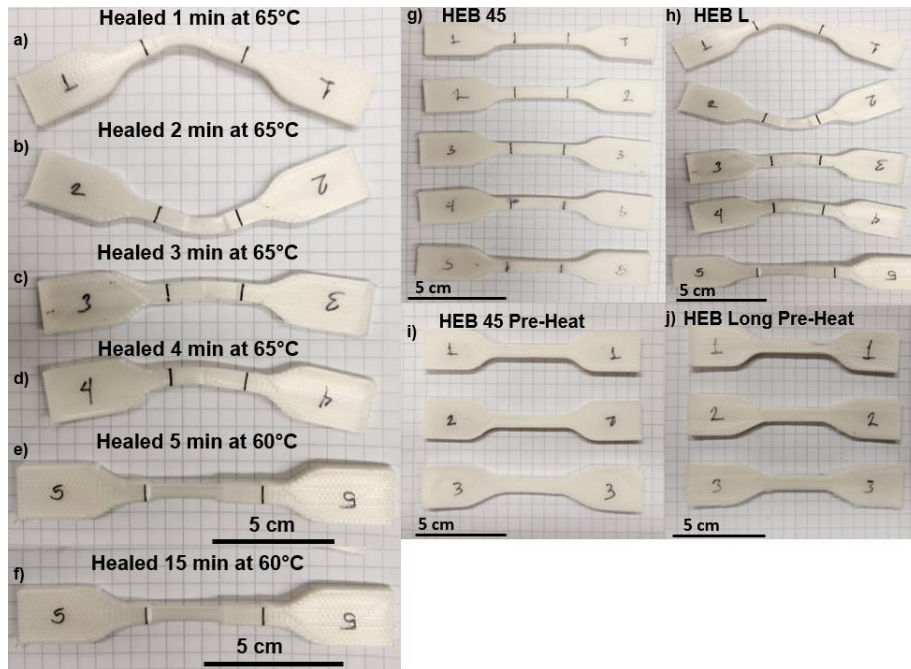Figure 3.5. Shape Memory Test regular blends.

Figure 3.6. Shape Memory Test HEB with different times (a,b,c,d,e,f) and baseline (g,h) vs pre-heated (i,j).

The comparison of all blends with their shape memory properties was compiled and presented in Figure 3.7, where the behavior of all blends used in this study is

compared to one an another. As it can be seen the best behavior was obtained by the HEB was the most stable blend overall of all while the Type V specimens made from 50/50 PCL/ TPU were the blend that did not performed very well during the study for not maintaining its shape however its recovery ratio is the best out of the binary blends is comparable with the Type IV 50/50 PCL/TPU and can be somewhat matched with the HEB blends. The blends that surpass the 1.0 line means that they had shrinkage as stated before. On Figures Figure 3.8 Figure 3.9 Figure 3.10 Figure 3.11 Figure 3.12 the SMP can be seen
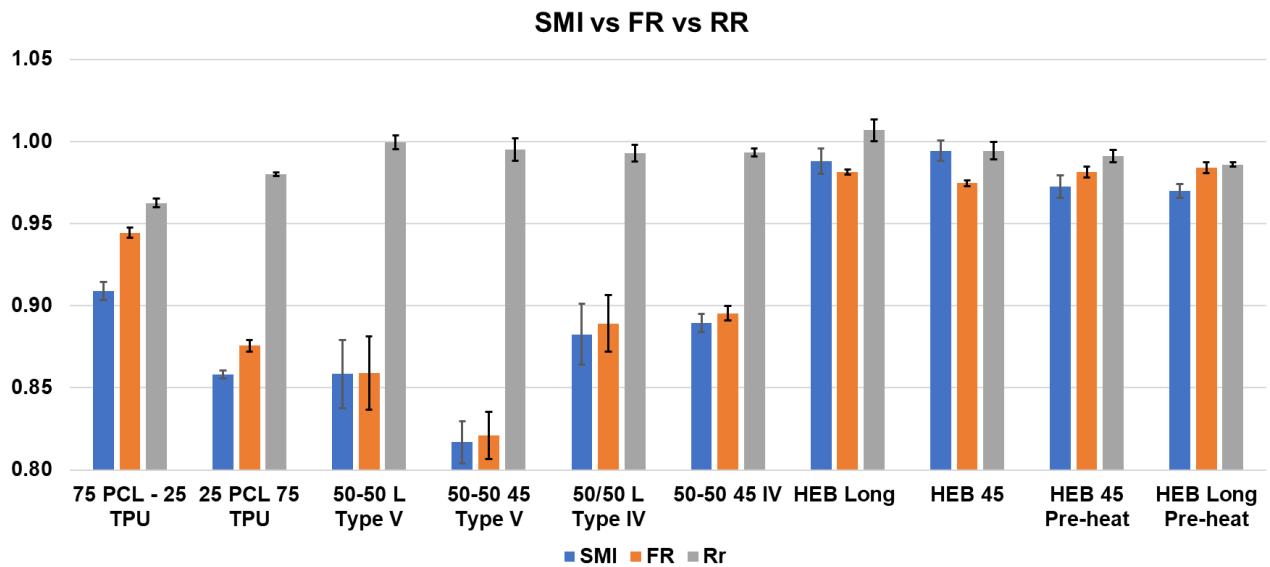

Figure 3.7: Shape Memory Index/ Fixation Ratio/ Recovery Ratio comparison.
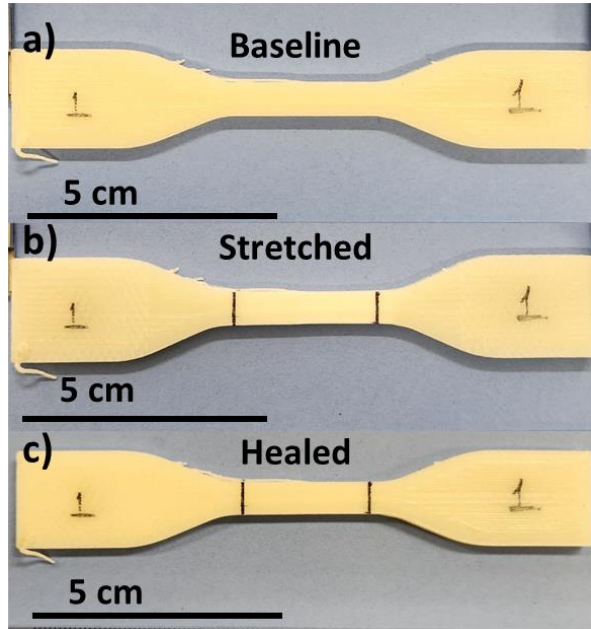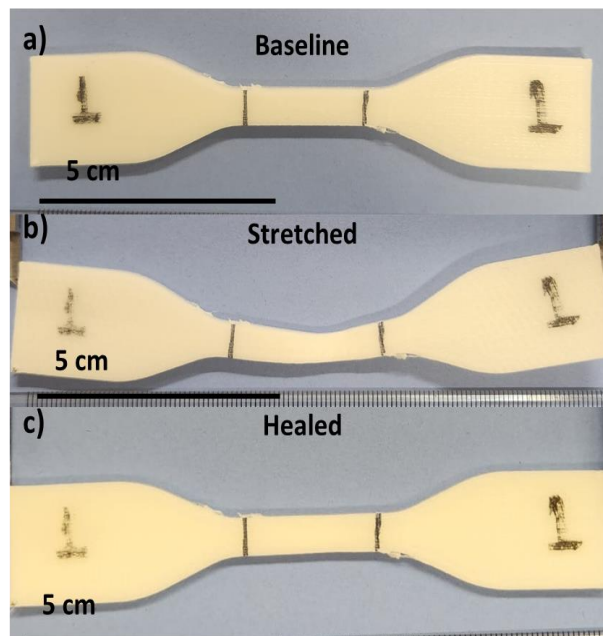
Figure 3.8: Shape Memory Test Process 25 PCL 75 TPU
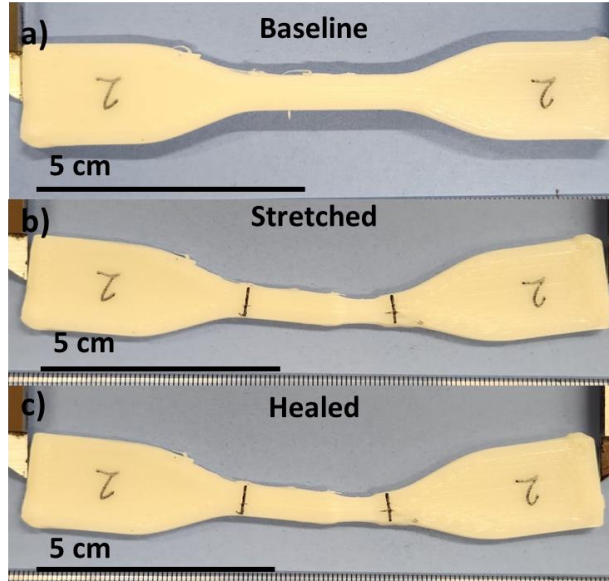

Figure 3.9:Shape Memory Test Process 50 PCL 50 TPU
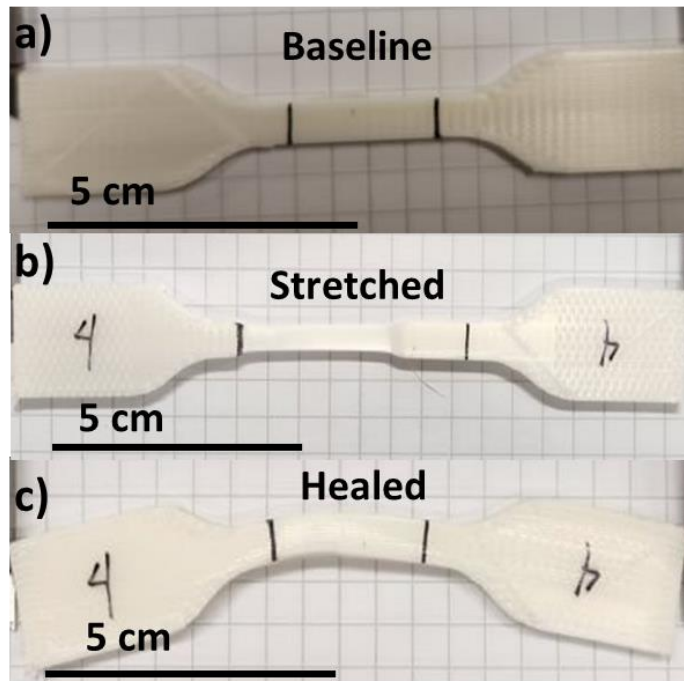
Figure 3.10: Shape Memory Test Process 75 PCL 25 TPU
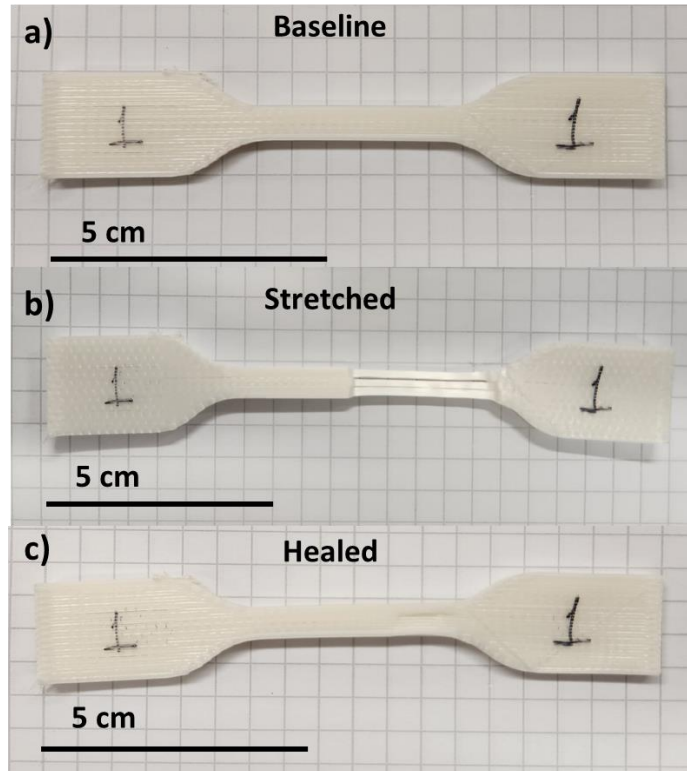

Figure 3.11: Shape Memory Test Process HEB Long

Figure 3.12: Shape Memory Test Process HEB Pre-Heated

SELF-HEALING EFFECT TESTING

The first method we used to evaluate the self-healing aspects of our material systems was to pull the specimens to failure after they were subjected to a shape memory test cycle to evaluate how the materials responded to damage. We have found this to be a useful method in determining what is effectively resiliency of the material [25]. During this test we could observe the output of the HEB and how it could heal in a same manner as the 50/50 PCL/TPU blend as seen in however in terms of elongation the HEB 45° orientation healed better than the 50/50 PCL/TPU 45° Orientation, as it is shown in Figure 3.13.
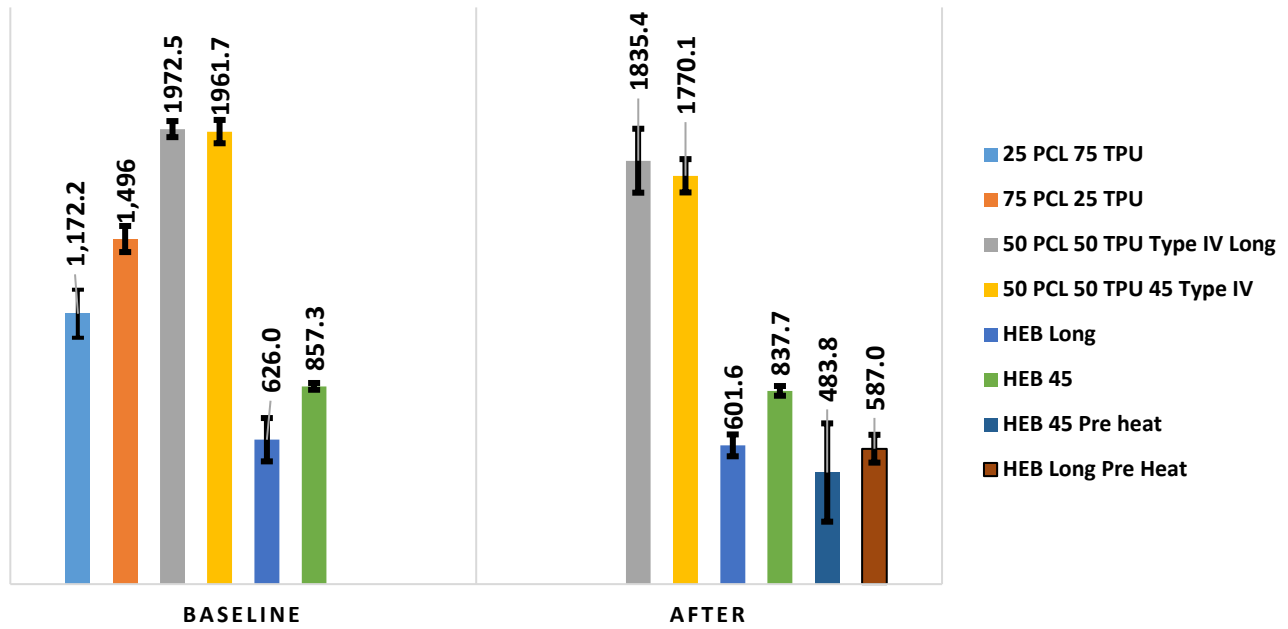
% ELONGATION BASELINE VS AFTER SMT

Figure 3.13: Elongation Baseline vs After SMT

On Figure 3.14 the tensile specimens' UTS can be observed, and it can be clearly seen that after the shape memory test (SMT) the strongest blend now was 50/50 PCL/TPU with longitudinal elongation in addition it even performed better than its regular blend and this only happened on this blend, the comparison can be spotted in Figure 3.13 and on this orientation so it can be inferred that it underwent a polymer relaxation process [47].
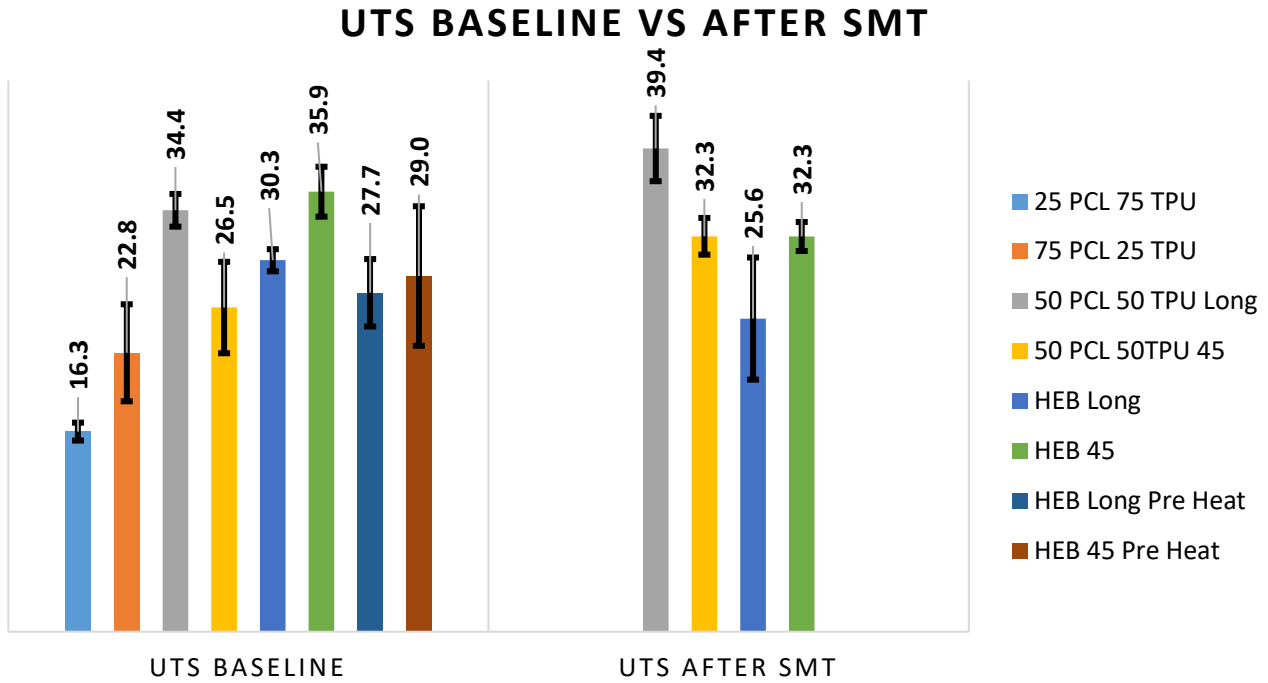
UTS BASELINE VS AFTER SMT

Figure 3.14: UTS Baseline vs After SMT

A qualitative test was developed where thin (0.4mm in thickness) specimens of material were printed, folded into random shapes and then recovered in water. The test was conducted using water at 68 °C and both raster patterns from the HEB were the main subjects. The self-healing process was successfully conducted since both patterns recovered as seen in Figure 3.15. Upon folding the specimens exhibited craze cracking, which is indicative of material damage. The film recovered its shape and little to no craze cracks were observed after testing (Figure 3.15 c and e). The film was folded 3 times in 45° orientation and 2 times in longitudinal at room temperature and was recovered in less than 5 seconds and the shape returned to its original form. In Figure 3.16 the 45° orientations can be observed, and it did not got as curled as the longitudinal raster specimen. This shape is obtained presumably due to deformation at the moment the specimen is taken from the print bed it gets a curled shape not a completely flat shape as

it seen in the Figure 3.15 a. The longitudinal pattern got a rounder shape after it was taken out of the printer as seen in Figure 3.17 d, both materials recovered well however, the longitudinal morphed into a curled shape inside the water as it is seen in Figure 3.17 d after being in the water for about 4 seconds after its shape recovery which may indicate a secondary shape memory effect.
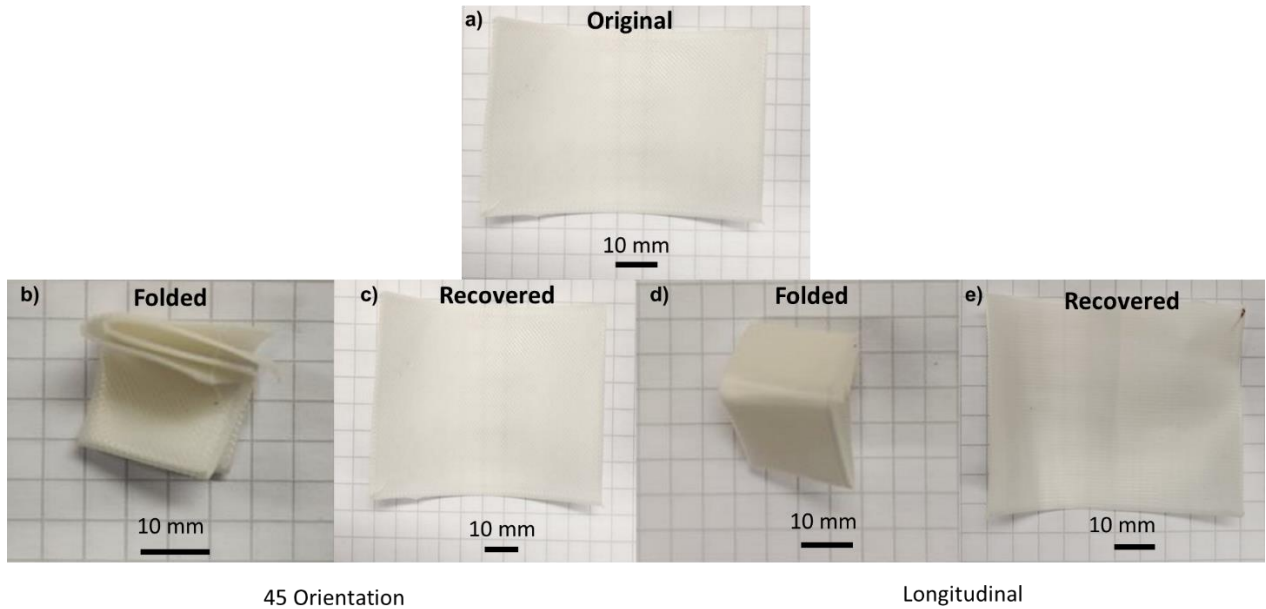

Figure 3.15. Self-Healing effect in HEB Long (b/c) and 45 Orientation (d/e).
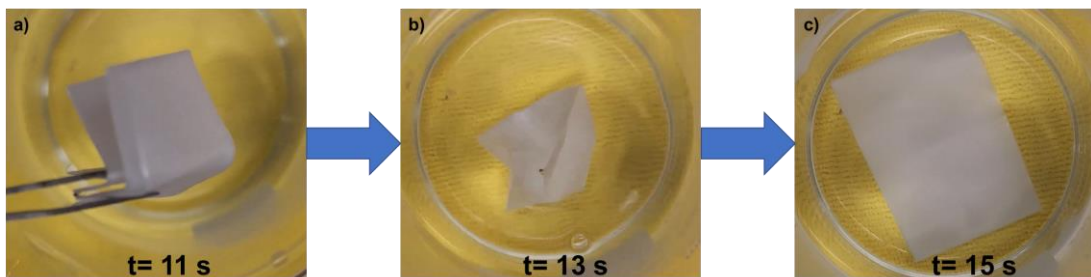

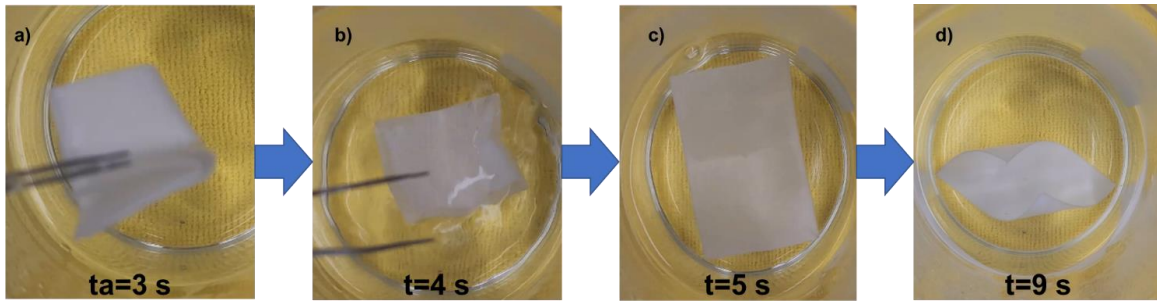Figure 3.16. Self-Healing 45° Raster pattern effect in video.

Figure 3.17. Self-Healing longitudinal Raster pattern effect in video.

A cut test was conducted as well and compared the behavior of the 50/50 PCL/TPU and HEB with both raster patterns for this test. The experimental set up influenced the test and it was difficult to actually use the fixture described in Methods section to create an ideal self-healing environment. Despite these difficulties, the 50/50 PCL/TPU binary blend successfully healed after 5 min at 80 °C, as it can be shown in Figure 3.18 where image a) is the specimen before cut, b) is the specimen after cut c) and d) is after the type V is healed and in d) the specimen was imaged being held from the top and it did not fall down, this happened in both raster patterns however, the bond was not strong enough to be tested in the tensile test machine as when it was placed for the test it would snap.

This effect could be because of the jig that was used that did not have enough thermal conductivity along the specimen however, is a notable finding that the 50/50 PCL/TPU is able to recover from a whole cut. In Figure 3.19 the specimen can be seen under the microscope and how the rupture healed after removing the specimen from the fixture. This result could be because of the set-up of the self-healing process or even the mold release (cooking spray) and the amount of PCL in the blend.it was recovered in the oven. In Figure 3.20 the 45° orientation can be spotted and healed as well.

On the other hand, the HEB could not be healed during any of the test with any of the raster pattern, the conditions were the same as the previous blend but at the moment of taking it out from the jig it would snap and break. The specimen was not able to make

27

it through the damage it already received. The mold release could be a reason due to its propagation through the crack and could prevent the fibers from recovering themselves and as well as the set up since the FFF is not exact and the jig did not fit exactly as it needed to be. Moreover, the PLA or the low content of PCL could be preventing the properties of self-healing to react to the temperature.
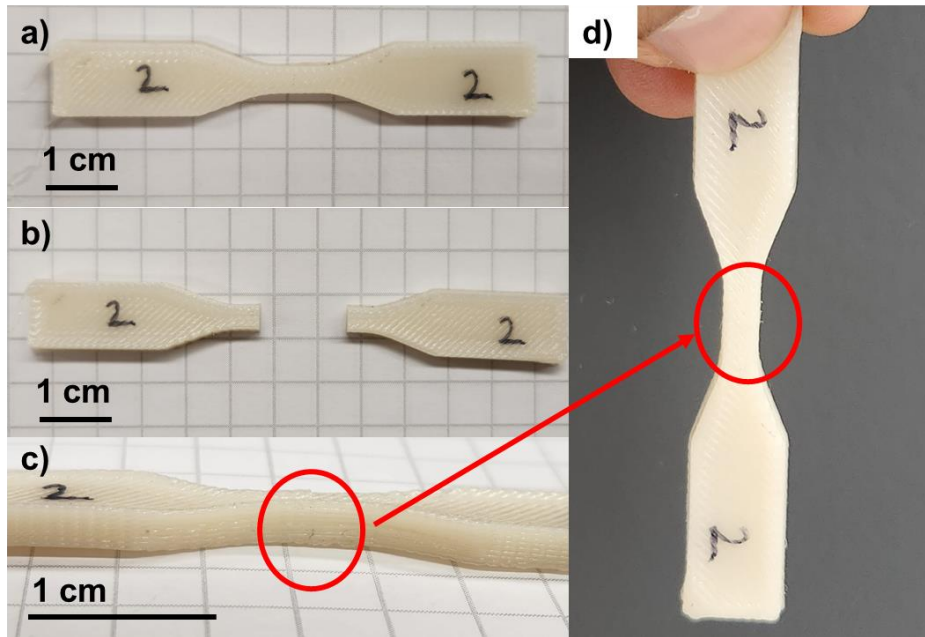
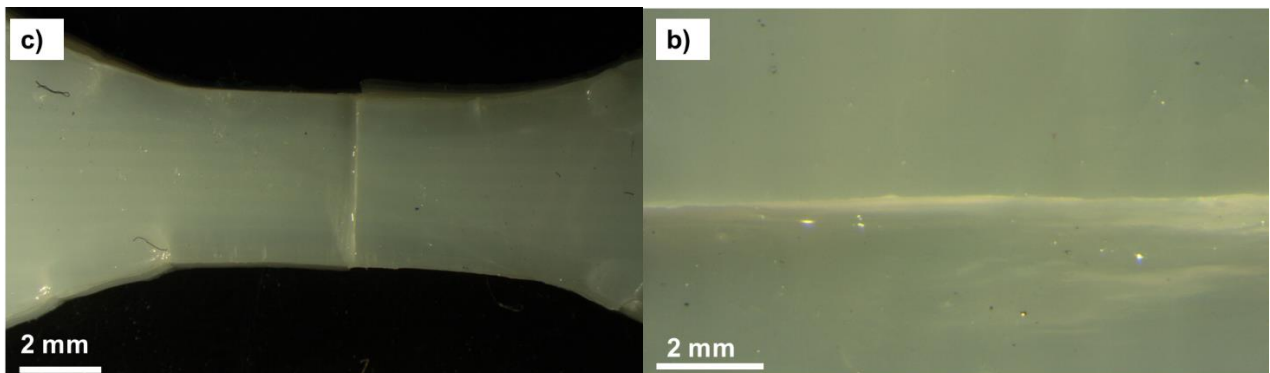

Figure 3.18: 50/50 PCL/TPU Cut test
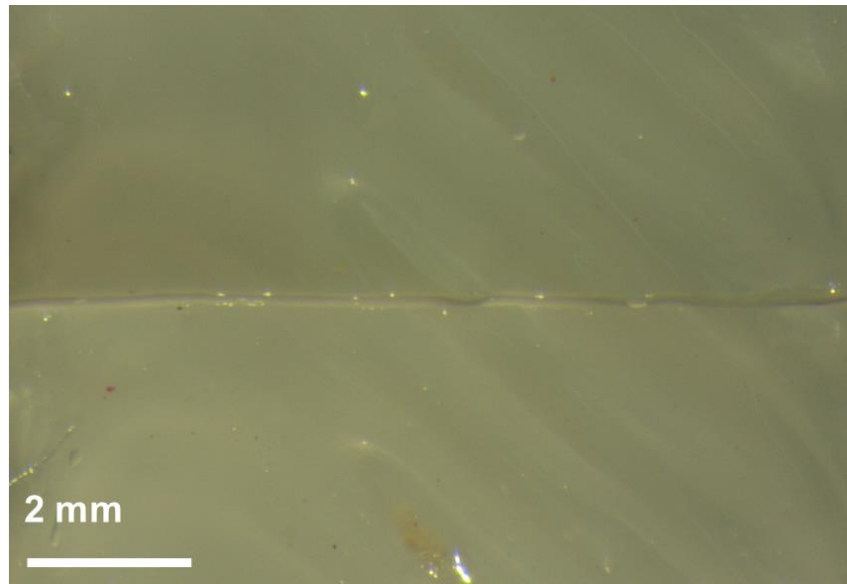

Figure 3.19: Type V Healed

Figure 3.20: Type V Healed 45° Orientation

SEM ANALYSIS

During the SEM analysis different features were compared between the two blends that stand out from the rest (50/50 PCL/TPU and HEB). There were some differences that were announced. In Figure 3.21 the 50/50 PCL/TPU 45° orientation can be observed clearly in the red circle the formation of the layering when it was printed as well as the plastic deformation is present and how the brittle fracture formed during the tension testing. There are some dimples and voids and a channel like feature that could be a fiber that tore before the complete fracture of the specimen. Elongation of fibers are spotted as well in the picture and the deformation of the fibers. Due to the nature of the pull, there is no delamination failure.
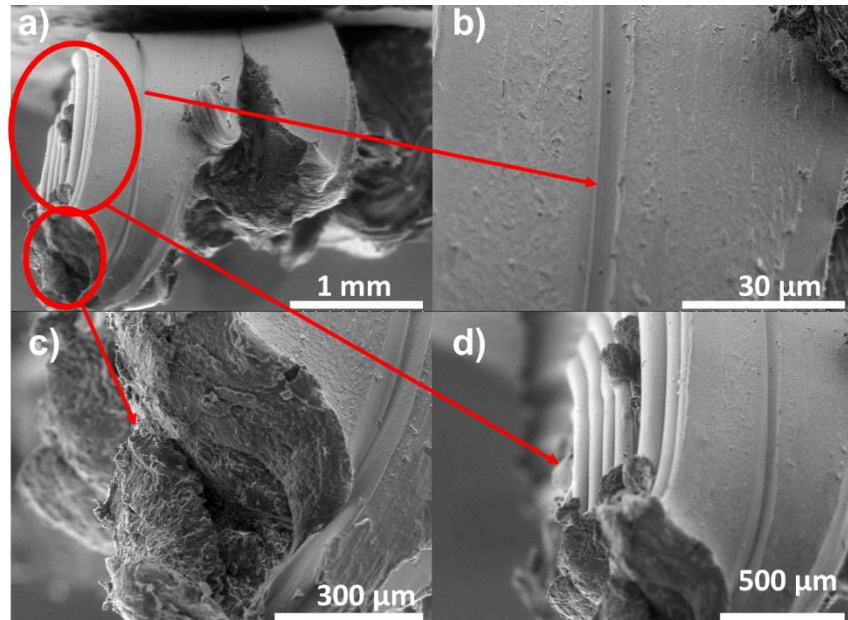
Figure 3.21. 50/50 PCL/TPU 45 SEM Fracture Surface.
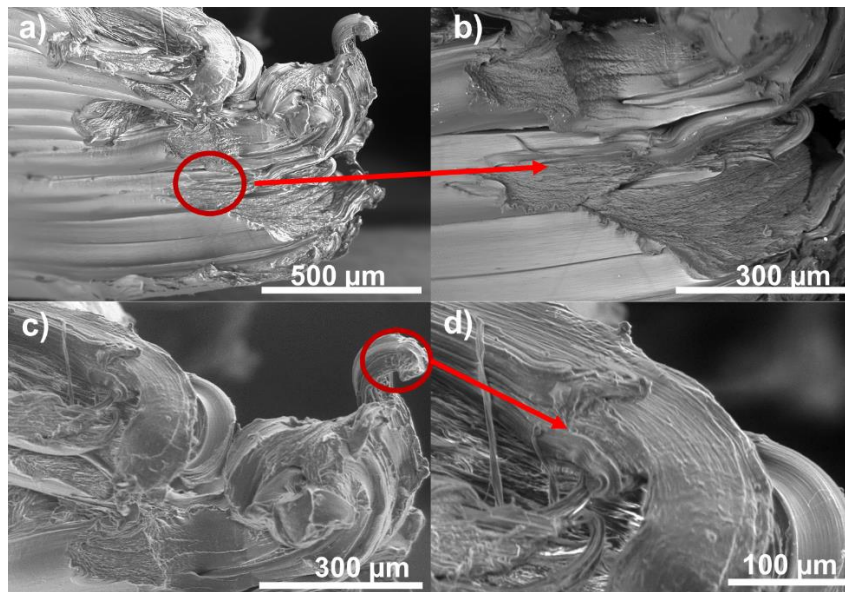
Figure 3.22. 50/50 PCL/TPU Longitudinal SEM Fracture Surface.

In Figure 3.22 the 50/50 PCL/TPU longitudinal specimen is present, in this picture there are more ductile failure presence than in the 45° orientation. The main reason is the printing orientation that would make the sample more ductile than the 45° however in the image b) of the Figure 3.22 the arrow indicates a brittle fracture mode that was present at the moment of the fracture this means that when it fractured it was an instant failure.

In Figure 3.23, is where the HEB starts to see its failure mode. In contrast with TPU and PCL blend the HEB showed a more brittle fracture mode. The delamination of the specimen can be spotted in this blend and this could be due to the printing parameters and the possibility of lack of temperature during the printing process this could be inferred by looking at the image "a" and "b" in the bottom the layers can be spotted to be more uniform stacked than the top layers and this could be due to the bed temperature. Besides, the fibers also present evidence of brittle fracture surface as can be seen in the image "d" of figure 17 where there is a "clean" cut and there is no evidence of elongation or dimples. In Figure 3.24, can be spotted that there was not that ductile fracture in the image b there are evidence of brittle fracture and on image a and c only can be seen some spots of elongation of the fibers so the fracture mode can be defined as mixed in this blend as well.
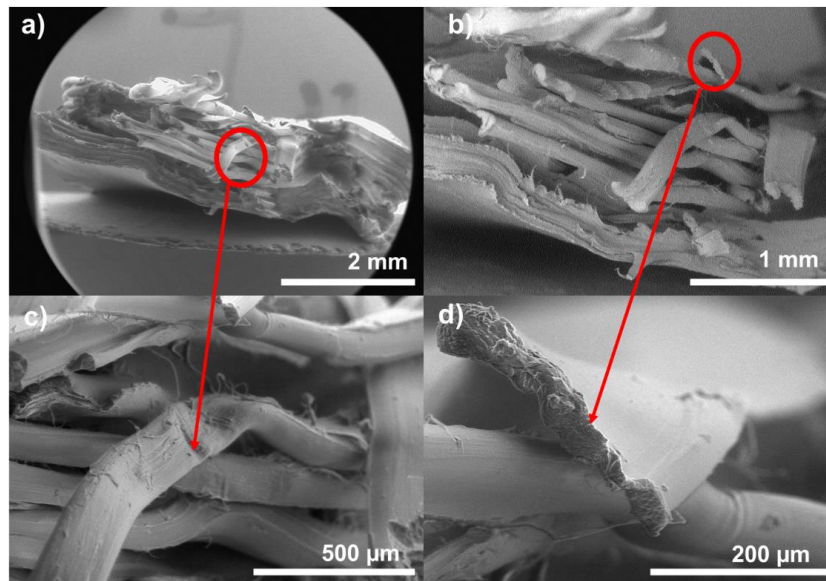
Figure 3.23. HEB Longitudinal SEM Fracture Surface.
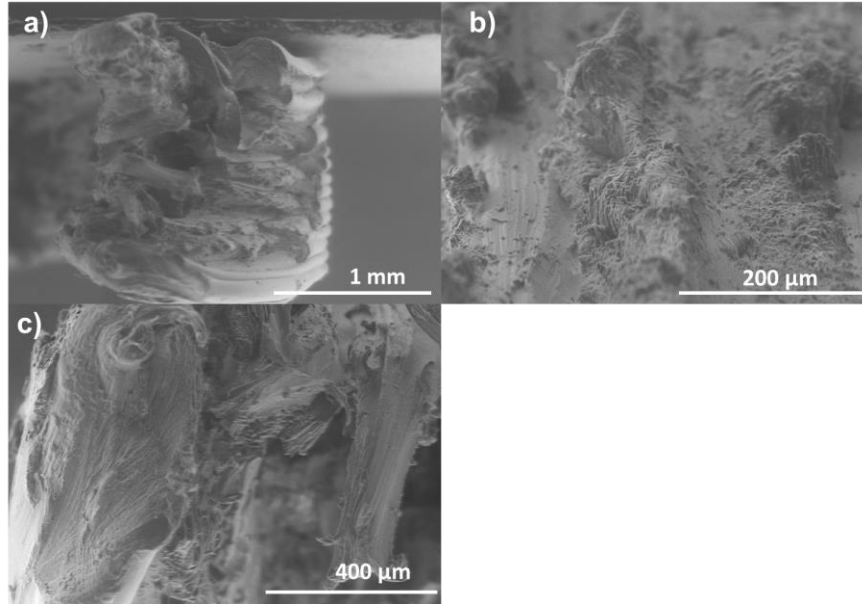
Figure 3.24. HEB 45 SEM Fracture Surface

In Figure 3.25 and Figure 3.26, it can be seen there in fact there was some difference between the pre-heat samples and no pre-heated samples. In contrast with the 45° HEB, here it can be seen that the layers are homogenized better and there are no big gaps between them the fracture surface is more ductile than the previous one and this would be due to the material is more compacted. However, it does not look as ductile as the 50/50 PCL/TPU Blend.
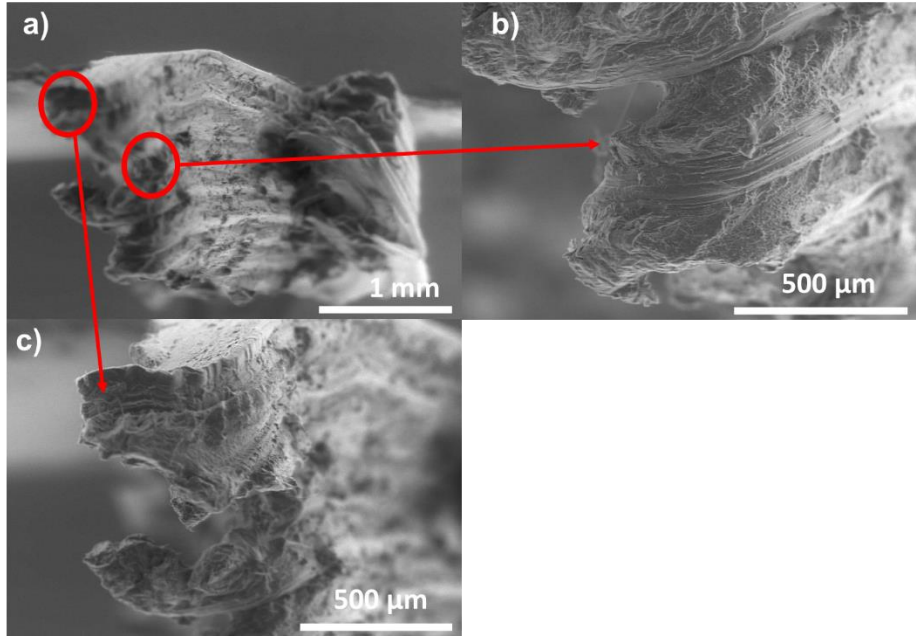
Figure 3.25. HEB 45° Pre Heat SEM Fracture Surface.
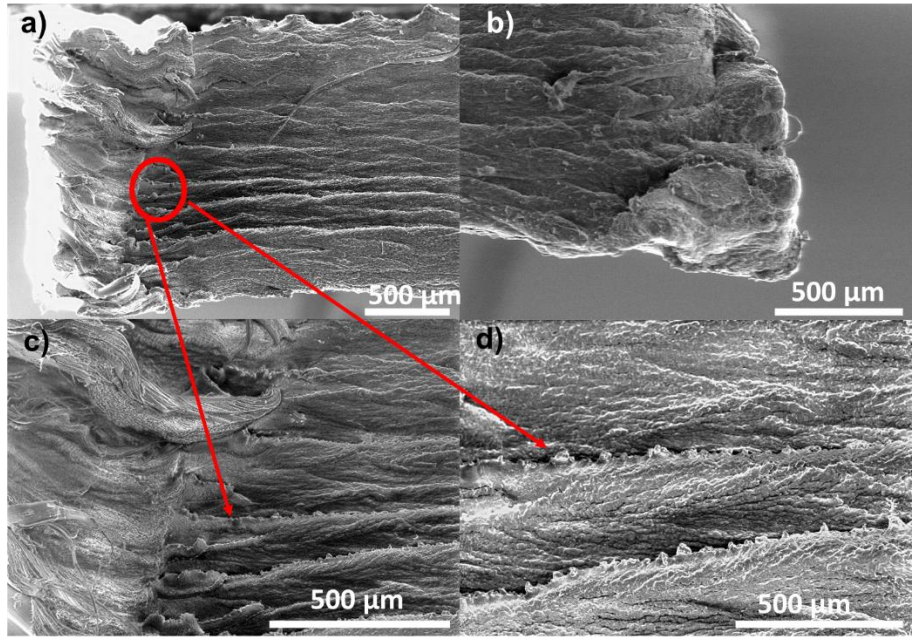
Figure 3.26. HEB Longitudinal Pre-Heat SEM Fracture Surface.

4. Microtome Analysis

A study was conducted using the cryo-microtome machine to look at the phases of the HEB blends, in Figure 4.1 the images can be spotted and the phases can be differentiated in the red circles. This images allow us to comprehend better the material and look that there polymers were able to blend together.

In Figure 4.2 the two phases are observable, which is a notable finding as there are three constituents in the HEB.
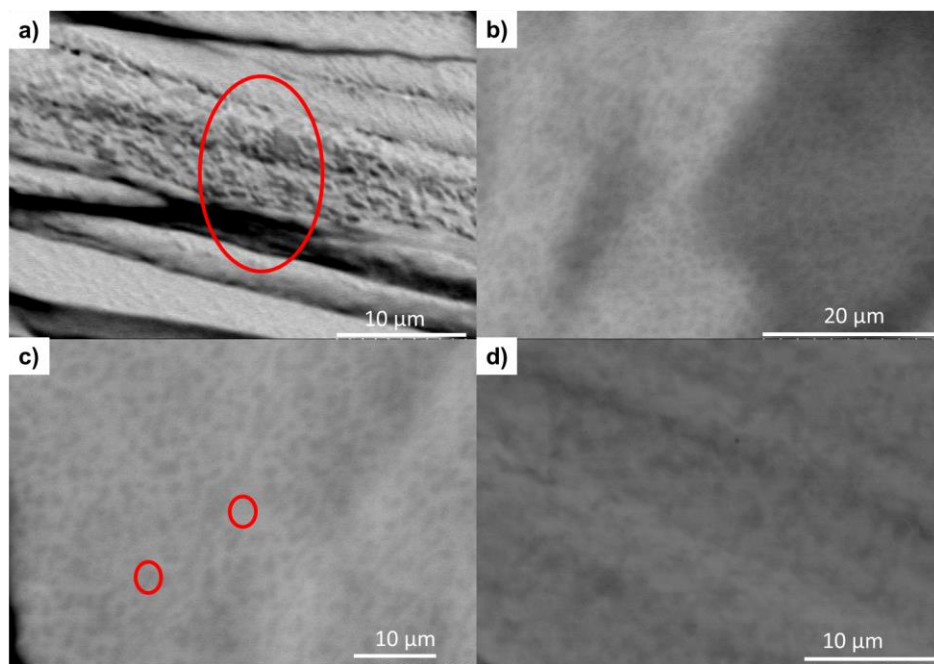
Figure 4.1: Microtome HEB
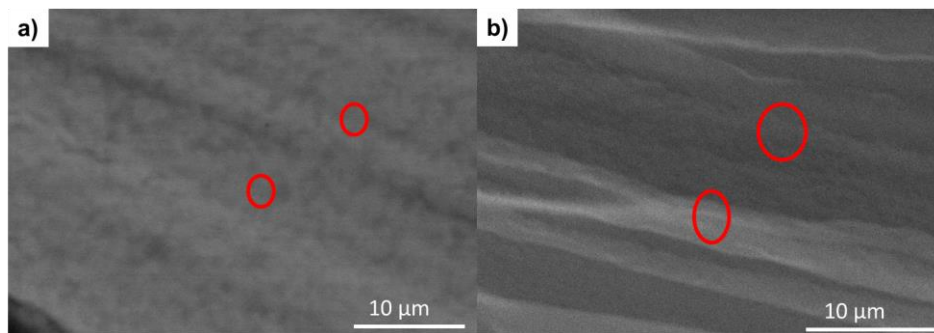
Figure 4.2: Microtome HEB

5. Chapter 4: Summary and Conclusions

The work presented here demonstrates an iterative design sequence for the melt compounding of polyesters with the long-term goal of creating high entropy polymer systems with shape memory and self-healing capabilities. Utilizing a materials selection strategy based on solubility parameter values, polymer type, and molecular geometry, binary blends composed of PCL and TPU and a ternary blend composed of PCL, TPU, and PLA were created by way of melt compounding.

Initial testing of variations of the binary blend found that a high PCL content (75% by weight) was difficult to extrude and did not perform well both in terms of printability and physical properties. When the ratio was shifted to be a majority TPU (75% by weight), the %El values were surprisingly low and the UTS values were also lower. The blend of 50/50 by weight PCL/TPU exhibited the most robust physical properties The premise of equal parts led us to pursue a three-component system of equal parts, essentially a high entropy polymer blend. The PCL-TPU behavior caught the attention due on 50-50 binary blend and the results were investigated and diverse authors[48] [49] that state that the tensile strength may be affected by the crystallinity of the polymer due to crystallinity and PCL lamellar thickness influence the permanent deformation stress in addition that at constant temperature the soft segments face a decline in their conformational entropy[50].

Both materials were evaluated in terms of raster pattern as well as between themselves. Notable results were that the HEB did not display a raster pattern sensitivity between the two raster patterns tested. This phenomenon warrants more study. In the case of the binary blend, when comparing baseline tensile data to tensile specimens that

were tested after a shape memory cycle, a work hardening effect is observed as the UTS values are greater for cycled specimens and the %El values are lower. This phenomenon also warrants more study.

In terms of shape memory performance, the HEB performed better than the binary blend, however shrinkage was observed. This is most likely due to polymer relaxation that occurs during the printing process. An experimental set was pre-heated at the glass transition temperature of the blend prior to shape memory testing in an effort to de-relax the specimens and the superior shape memory properties were retained without specimen shrinkage.

Efforts to examine the microstructure of the polymer blend yielded limited results, but we were able to discern two distinct domains within the HEB specimen. This is noteworthy as there are three constituents in the blend. Though the data pertaining to self-healing in terms of cut specimens is also limited, the binary blend of PCL/TPU in a 50/50 ratio exhibits superior self-healing capabilities as compared to the HEB. This is most likely due to the higher PCL content which becomes tacky and potentially flows when heated.

There are still many questions to answer about High Entropy Blends or ternary blends since there is still a subject in development however, during this study it can be concluded that there are some aspects of the blends that these ternary blends can improve the binary blends such as their shape memory properties which they were stabilized when the PLA was added and, in some cases, tensile strength however there are other aspects where it does not behave better than the binary blends.

The printing parameters of the ternary blend (HEB) can be improved too due to there was not a complete fusion between the layering and that could be the reason why the pre-heated samples worked better in some mechanical aspects. The challenges still prevail in the additive manufacturing industry and some other printing techniques could be tested to see if that outcome is better than FFF and would be useful to test if it could be viable to use the blend as a scaffold for biomedical applications or even if a ligament or tendon can be built after this blend [51] and spot the differences among a binary blend and a ternary blend.

In conclusion 50% PCL 50% TPU got the best properties between all of the binary blends and its tensile properties do not depend on size however, their shape memory properties such as fixation ration and shape memory index do depend on the size. Compared to the HEB the 50/50 PCL/TPU behaved better in terms of elongation. Also, according to the SEM pictures the 50/50 PCL/TPU blend was more ductile than any of the ternary blends whether pre-heated or not pre-heated. On the other hand, HEB has more stable shape memory properties overall. The HEB showed a potential self-healing material that could be studied deeper since the material healed in the surface, but it did not reach the crosslink section, in the future different additives could be added in order to enhance this property due to the three polymers have the same solubility parameter. All of these properties could be enhanced by changing the PLA concentration due to this polymer tending to embrittle the mix or use a different mixing technique so the PLA can integrate better to the blend. The cut test is still in development and could be performed better with different tools that could make the blend heal in a better manner.

FUTURE WORK:

The recommendations for the future would include to experiment with different printing parameters to improve the adhesion between the printing layers and avoid the delamination that was present on Figure 3.23.

In respect to the binary blend, it would be a good option to compare with 45 PCL 55 TPU and vice versa to see the effect of each blend and figure out if it could improve its performance on tensile strength. And % elongation.

The next step would be to compare the HEB mechanical properties to tendons and ligaments in order to determine if it could be a good option for biomedical graft applications. The next recommendation will be the development of a standard to perform an accurate cut test that could guarantee a precise result and a tool to properly heal an specimen.

6. Chapter 5: References:

1. F. Andrade Chávez, J. G. Siqueiros, I. A. Carrete, I. L. Delgado, G. W. Ritter, and D. A. Roberson, Virtual and Physical Prototyping **14**, 188 (2019).

2. J. Delaey, P. Dubruel, and S. Van Vlierberghe, Advanced Functional Materials **30**, 1909047 (2020).

3. N. Sabahi, W. Chen, C.-H. Wang, J. J. Kruzic, and X. Li, JOM **72**, 1229 (2020).

4. P. A. Quiñonez, L. Ugarte-Sanchez, D. Bermudez, P. Chinolla, R. Dueck, T. J. Cavender-Word, and D. A. Roberson, Materials **14**, 4254 (2021).

5. D. Fico, D. Rizzo, R. Casciaro, and C. Esposito Corcione, Polymers **14**, 465 (2022).

6. H. Zhang, H. Wang, W. Zhong, and Q. Du, Polymer **50**, 1596 (2009).

7. Y. Wang, J. Zhang, M. Li, M. Lei, Y. Wang, and Q. Wei, J Polym Res **29**, 243 (2022).

8. D. Rahmatabadi, M. Aberoumand, K. Soltanmohammadi, E. Soleyman, I. Ghasemi, M. Baniassadi, K. Abrinia, M. Bodaghi, and M. Baghani, Advanced Engineering Materials **25**, 2201309 (2023).

9. X. Jing, H.-Y. Mi, H.-X. Huang, and L.-S. Turng, Journal of the Mechanical Behavior of Biomedical Materials **64**, 94 (2016).

10. X. Xu, P. Fan, J. Ren, Y. Cheng, J. Ren, J. Zhao, and R. Song, Composites Science and Technology **168**, 255 (2018).

11. D. Myers, A. Abdel-Wahab, F. Hafeez, N. Kovacev, and K. Essa, Journal of the Mechanical Behavior of Biomedical Materials **136**, 105447 (2022).

12. A. Aimar, A. Palermo, and B. Innocenti, Journal of Healthcare Engineering **2019**, e5340616 (2019).

13. F. Ebrahimi and H. Ramezani Dana, International Journal of Polymeric Materials and Polymeric Biomaterials **71**, 1117 (2022).

14. J.-W. Yeh, S.-K. Chen, S.-J. Lin, J.-Y. Gan, T.-S. Chin, T.-T. Shun, C.-H. Tsau, and S.-Y. Chang, Advanced Engineering Materials **6**, 299 (2004).

15. C. Haase, F. Tang, M. B. Wilms, A. Weisheit, and B. Hallstedt, Materials Science and Engineering: A **688**, 180 (2017).

16. V. V. Popov, A. Katz-Demyanetz, A. Koptyug, and M. Bamberger, Heliyon **5**, e01188 (2019).

17. Y. Huang, J.-W. Yeh, and A. C.-M. Yang, Materialia **15**, 100978 (2021).

18. T. Hirai, K. Yagi, K. Nakai, K. Okamoto, D. Murai, and H. Okamoto, Polymer **240**, 124483 (2022).

19. S. Wang and M. W. Urban, Nat Rev Mater **5**, 562 (2020).

20. C. C. Hornat and M. W. Urban, Progress in Polymer Science **102**, 101208 (2020).

21. D. Kong, J. Li, A. Guo, X. Zhang, and X. Xiao, European Polymer Journal **120**, 109279 (2019).

22. S. Su, mona duhme, and R. Kopitzky, Materials **13**, 4897 (2020).

23. K. Adamska, A. Voelkel, and A. Berlińska, Journal of Pharmaceutical and Biomedical Analysis **127**, 202 (2016).

24. R. Gallu, F. Méchin, F. Dalmas, J.-F. Gérard, R. Perrin, and F. Loup, Polymer **207**, 122882 (2020).

25. J. M. Avila, T. J. Cavender-Word, and D. A. Roberson, J Polym Environ (2023).

26. P. Quinonez, Open Access Theses & Dissertations (2019).

27. T. J. Word, A. Guerrero, and D. A. Roberson, MRS Communications **11**, 129 (2021).

28. S. Wang and M. W. Urban, Nat Rev Mater **5**, 562 (2020).

29. S. Bhattacharya, R. Hailstone, and C. L. Lewis, ACS Appl. Mater. Interfaces **12**, 46733 (2020).

30. S. J. Kalista Jr., in *Self-Healing Materials* (John Wiley & Sons, Ltd, 2008), pp. 73–100.

31. D. Y. Wu, S. Meure, and D. Solomon, Progress in Polymer Science **33**, 479 (2008).

32. P. Zhang and G. Li, Progress in Polymer Science **57**, 32 (2016).

33. R. P. Wool and K. M. O'Connor, Journal of Applied Physics **52**, 5953 (1981).

34. J. A. Syrett, C. Remzi Becer, and D. M. Haddleton, Polymer Chemistry **1**, 978 (2010).

35. Y.-L. Liu and T.-W. Chuo, Polymer Chemistry **4**, 2194 (2013).

36. S. Bode, M. Enke, M. Hernandez, R. K. Bose, A. M. Grande, S. van der Zwaag, U. S. Schubert, S. J. Garcia, and M. D. Hager, in *Self-Healing Materials*, edited by M. D. Hager, S. van der Zwaag, and U. S. Schubert (Springer International Publishing, Cham, 2016), pp. 113–142.

37. Z. Wang, X. Lu, S. Sun, C. Yu, and H. Xia, J. Mater. Chem. B **7**, 4876 (2019).

38. S. J. Garcia, European Polymer Journal **53**, 118 (2014).

39. H. Wu, H. Xie, X. Tian, Y. Sun, B. Shi, Y. Zhou, D. Sheng, X. Liu, and Y. Yang, Progress in Organic Coatings **159**, 106409 (2021).

40. S. Gupta, A. Sharma, J. Vasantha Kumar, V. Sharma, P. K. Gupta, and R. S. Verma, International Journal of Biological Macromolecules **162**, 1358 (2020).

41. (n.d.).

42. Y. Zhou, L. Luo, W. Liu, G. Zeng, and Y. Chen, Advances in Materials Science and Engineering **2015**, 1 (2015).

43. F. Liu, C. Vyas, G. Poologasundarampillai, I. Pape, S. Hinduja, W. Mirihanage, and P. Bartolo, Macromolecular Materials and Engineering **303**, 1700494 (2018).

44. AMFG, AMFG (2018).

45. J. G. Siqueiros and D. A. Roberson, International Journal of Polymer Science **2017**, 1954903 (2017).

46. R. G. Ferrillo and P. J. Achorn, Journal of Applied Polymer Science **64**, 191 (1997).

47. R. D. Priestley, C. J. Ellison, L. J. Broadbelt, and J. M. Torkelson, Science **309**, 456 (2005).

48. Biomaterials **26**, 4219 (2005).

49. N. Lee, Shape Memory Property of PCL/TPU Blends with a Diisocyanate Compatibilizer, Kocaeli Üniversitesi, Fen Bilimleri Enstitüsü, 2018.

50. E. Aboueimehrizi, M. A. Makaremy, S. Bazrpash, F. Noormohammadi, Y. R. Darestani, and M. Nourany, Cellulose **29**, 8651 (2022).

51. B. B. Kang, H. Lee, H. In, U. Jeong, J. Chung, and K.-J. Cho, in *2016 IEEE International Conference on Robotics and Automation (ICRA)* (2016), pp. 3750–3755.

Vita

My name is Luis Eduardo Lares Carrillo born and raised in Ciudad Juárez, I got my bachelor's degree in industrial and Systems Engineering in the Universidad Autónoma de Ciudad Juárez. I worked in the maquiladora industry for over 7 years, this manufacturing industries were automotive and medical and I worked as Engineer for a medical device company for over 4 years, after that and started my Master's degree in Metallurgy and Materials Engineering in the University of Texas at El Paso. During that time, I was a commuter student and worked as an Engineer at Johnson & Johnson which manufactures medical devices.

On 2021 I started working as a Teaching Assistant for the department of Metallurgy, Materials and Biomedical Engineering and helped the professors and students to be able to learn the subjects across the different programs in the department. During summer 2022 I was enrolled to the AFRL to guide high school's students to create an Engineering project and it was a complete success since some of them were very interested in the field and even enrolled to the program.

During my stay at UTEP I was able to get to know the materials structure and many techniques and focus on 3D printing (FFF) technique of different polymers. I also could work with some metals and learn its applications.

Contact Information: <;lares.luis@outlook.com>